Height correction of atmospheric motion vectors using airborne lidar observations

Martin Weissmann, Kathrin Folger and Heiner Lange

Hans-Ertel-Centre for Weather Research, Data Assimilation Branch, Ludwig-Maximilians-Universität München, Germany

Manuscript submitted to the *Journal of Applied Meteorology and Climatology*

August 2012

Corresponding author address:

Martin Weissmann,

LMU München, Meteorologie,

Theresienstr. 37,

80333 Munich, Germany

E-Mail: martin.weissmann@lmu.de

ABSTRACT

Uncertainties in the height assignment of Atmospheric Motion Vectors (AMVs) are the main contributor to the total AMV wind error and these uncertainties introduce errors that can be horizontally correlated over several hundred kilometers. As a consequence, only a small fraction of the available AMVs is currently used in numerical weather prediction systems. For this reason, we investigate how to improve the height assignment of AMVs, at first with independent airborne lidar observations and secondly by treating AMVs as layer-winds instead of winds at a discrete level.

The lidar-AMV height correction reveals that the wind error of AMVs can be reduced by 5-10% when AMV winds are assigned to a 100-150 hPa deep layer beneath the cloud top derived from nearby lidar observations. The correction is performed using airborne lidar observations during the THORPEX Pacific Asian Regional Campaign 2008, but the method could also be applied using satellite-based lidars. In addition to the reduction of AMV errors, the lidar-AMV height correction is expected to reduce the correlation of AMV errors as lidars provide independent information on cloud top heights.

Furthermore, AMVs are compared to dropsonde and radiosonde winds averaged over vertical layers of different depth to investigate the optimal height assignment for AMVs in data assimilation. Consistent with previous studies, it is shown that AMV winds better match sounding winds vertically averaged over ~100 hPa than sounding winds at a discrete level. The comparison to deeper layers further reduces the RMS difference, but introduces systematic differences of wind speeds.

1. Introduction

Atmospheric Motion Vectors (AMVs) derived by tracking the drift of cloud or water vapor features in satellite imagery are a key element of the global observing system for the initialization of numerical weather prediction (NWP) models. They particularly constrain the wind field in remote areas of the southern hemisphere and above the world's oceans where hardly any other wind observations exist. Several studies have documented the positive contribution of AMVs to the forecast skill of global NWP models (Bormann and Thépaut 2004; Velden et al 2005; Gelaro et al. 2010). All major NWP centers now assimilate AMVs from several geostationary and polar orbiting satellites that together provide a nearly global coverage.

Despite improvements of the retrieval algorithms over the last decades however, the height assignment of AMVs introduces significant errors. Velden and Bedka (2009, VB2009 hereafter) estimated that the height assignment is the dominant factor in AMV uncertainty and contributes up to 70% of the total error. In addition, those errors are horizontally correlated over up to 800 km (Bormann et al. 2003). As a consequence, AMVs are usually thinned rigorously for the assimilation in NWP models. The European Centre for Medium-range Weather Forecasts (ECMWF) for example currently uses less than 10% of the available AMVs to avoid correlated errors.

Spaceborne lidars as the one on the Cloud-Aerosol Lidar and Infrared Pathfinder Satellite Observation (CALIPSO) satellite can accurately determine the height of cloud tops. Therefore, the combination of AMVs with cloud top information from satellite lidars is seen as promising approach to reduce the error and error correlation of AMVs. Di Michele et al. (2012) compared the cloud top heights derived from CALIPSO lidar data and AMV heights, but they didn’t correct AMV heights and they didn’t answer the question if the AMV should actually be assigned to the lidar observed cloud top itself or to some layer around or beneath the lidar cloud top observations.

The present study intends to develop a height correction for AMVs based on lidar observations. Instead of satellite lidar observations, the height correction is tested with airborne lidar observation during the THORPEX Pacific Asian Regional Campaign (T-PARC) 2008 (Weissmann et al. 2011, 2012). The use of airborne observations has the advantage that more than 300 dropsondes are available to validate AMV winds before and after the correction. Observations of the lidar backscatter ratio at 1064 nm and dropsondes were both performed during 24 research flights of the Falcon 20 research aircraft of the Deutsches Zentrum für Luft- und Raumfahrt (DLR).

In addition, the present paper investigates the appropriate layer depth and its vertical position for the assimilation of AMVs. The study of VB2009 indicates that AMVs represent the wind in a tropospheric layer rather than at a finite level. For this reason they calculated the vector root-mean-square (VRMS) difference between AMVs and radiosonde winds averaged over layers of different depth from the AMV height downward. The present paper also investigates the effect of layer-averages on the wind speed bias as systematic errors are particularly crucial in data assimilation. Furthermore, we test different vertical positions of the averaging layer relative to the original AMV height. For this reason we compare AMVs to sounding winds averaged over layers of different depth and we shift these layers from above to beneath the AMV. Systematic wind speed differences are calculated in addition to VRMS differences as deeper layers lead to systematically weaker winds. The comparison is based on several thousand vertical soundings (dropsondes and special radiosondes from ships and small islands) during T-PARC.

The paper is outlined as follows: Section 2 describes T-PARC and the data set. Section 3 first compares AMV heights to lidar cloud top heights and then evaluates an AMV height correction using lidar observations. Section 4 compares AMVs to layer-averaged radiosonde and dropsonde winds and section 5 summarizes the results.

2. Data set

a. T-PARC observations

The summer component of the multinational T-PARC field campaign was conducted in August to October 2008 in the western North Pacific. T-PARC and the associated projects Tropical Cyclone Structure 2008 (TCS-08) and Dropwindsonde Observations for Typhoon Surveillance near the Taiwan Region (DOTSTAR) aimed to investigate the genesis of tropical cyclones (TCs), to improve typhoon track and intensity forecasts by targeted observations and to investigate the extratropical transition of TCs and their downstream impact in midlatitudes (for more information see: http://www.eol.ucar.edu/projects/t-parc/). The main observational platforms were four research aircraft launching dropsondes: The German DLR Falcon 20, the U.S. Navy P-3, U.S. Air Force WC-130 and the Taiwanese DOTSTAR Astra Jet. Altogether, over 500 flight hours were spent and over 1300 dropsondes were launched in a period from 1 August to 3 October 2008. In addition to dropsondes, additional radiosondes were launched from Japanese research vessels and from small islands. The right panel of Fig. 1 shows the location of radiosondes and dropsondes used for the comparison of AMVs with layer-averaged sounding winds in section 4.

The DLR Falcon was additionally equipped with a scanning wind lidar and a differential absorption lidar (DIAL) system for water vapor observations (Wirth et al. 2009; Harnisch et al. 2011). As a byproduct of water vapor profiles, the DIAL system also observes vertical profiles of the backscatter ratio (*BSR)* at 1064 nm beneath the aircraft. These profiles can be used to accurately determine the height of cloud tops. After testing different approaches for deriving cloud top heights, the maximum of the *BSR* gradient plus a threshold for the *BSR* gradient were used for cloud detection. There are many different approaches for deriving cloud tops from lidar observations, but in general it was found that the differences between cloud heights derived using different approaches or slightly modified thresholds are clearly smaller than the differences between lidar cloud top heights and AMV heights (see Folger 2012 for details of the applied cloud detection method and differences of different approaches). The DLR Falcon performed 24 research flights with dropsonde and lidar *BSR* observations during T-PARC (Fig. 1). After quality screening, about 50 flight hours with lidar *BSR* observations were available for the AMV height correction.

The Cooperative Institute for Meteorological Satellite Studies (CIMSS) produced hourly AMVs from images of the operational Japanese Multi-functional Transport Satellite 1R (MTSAT-1R) in four channels: (1) infra-red (IR) observations at 10.8 µm; (2) visible (VIS) observations at 0.73 µm for daytime low clouds; (3) shortwave infra-red (SWIR) observations at 3.75 µm for nighttime low clouds; (4) observations in a channel sensitive to water vapor. The present study uses AMVs in the first three channels (IR, VIS and SWIR) that track clouds features. AMVs derived in the water vapor channel also track water vapor features and were therefore not used in the present study. The CIMSS algorithm for deriving AMVs is close to that used operationally by the National Environmental Satellite, Data, and Information Service (NESDIS) of the National Oceanic and Atmospheric Administration (NOAA). AMV heights were determined using H2O intercept method, the IR histogram method, and the cloud base method (see Nieman 1993 and Olander 2001 for more details).

The mean flight level of the DLR Falcon was 11 km ASL, but lidar cloud observations within 150 hPa from the aircraft downward were not used to assure that no AMVs from clouds above the aircraft with a lower erroneous height assignment are in the data set. Due to this selection criterion and a minimum of the number of cloud AMVs in the middle troposphere, only AMVs beneath 500 hPa are used for the height comparison and height correction. As a consequence, only AMVs derived from water, but not from ice clouds are in the data set. About 58% of these AMVs are VIS, about 25% are SWIR and 17% are IR (Fig. 2). The low fraction of IR AMVs is due to the fact that those are mainly located at higher altitudes. SWIR AMVs are only derived during nighttime, whereas most flights were performed during daylight.

b. Selection criteria for observations

Observations for the lidar-AMV height comparison and correction in section 3 were selected with the condition that there is a lidar cloud observation and an AMV within 60 min time difference and 100 km horizontal distance. CIMSS also provides a quality indicator (QI) for AMVs that ranges from 0-100 with 100 indicating the highest quality. This QI must be at least 50 for observations used in section 3. These thresholds were chosen to exclude lidar observations and AMVs from different clouds without reducing the sample size too much.

In addition, the height comparison in section 3a applied the criterion that the AMV height and the lidar cloud top must be within 150 hPa vertically to discard values where AMVs and the lidar cloud signal come from clouds at very different heights due to the temporal or horizontal displacement of the observations.

For the AMV height correction using lidar observations in section 3b, the pressure difference criterion was replaced by the criterion that the applied height correction is not more than 100 hPa, i.e. the center of the layer that the AMV is shifted to must be within 100 hPa from the original AMV height. These criteria are based on the assumption that AMV height errors are usually less than about 100-150 hPa, but were also based on sensitivity studies with different limits and the visual comparison of lidar *BSR* cross-sections and AMV heights. The evaluation of the lidar-AMV height correction was performed with wind observations from the two nearest dropsondes released by the DLR Falcon (one dropsonde for the first and last observations on a flight). For this evaluation, the additional criterion was applied that there is at least one dropsonde within 100 km and 60 min from the AMV and the lidar observation used for the correction.

The comparison of AMVs to layer-averaged radiosonde and dropsonde winds in section 4 applied the same threshold for temporal and horizontal displacement that was used in section 3 (100 km and 60 min), but the threshold for the CIMSS QI was increased to 70 as the data set was significantly larger and therefore allowed a more rigorous limit. Altogether 13,000 matches of AMVs and sounding winds could be used in section 4.

3. Lidar-AMV height comparison and correction

a. Height comparison

The histogram of height differences between AMVs and lidar cloud tops is shown in Fig. 3. The distribution strongly depends on the AMV type. VIS AMVs are distributed throughout the vertical range of +/- 150 hPa from the lidar cloud top height with more AMVs above than beneath the lidar cloud top. The majority of IR AMVs and nearly all SWIR AMVs in contrast are located beneath the lidar cloud tops. On average, the pressure of VIS AMVs is 19 hPa lower than at the lidar cloud tops, which means that VIS AMVs are on average located higher than the lidar cloud tops. The pressure of IR AMVs is 14 hPa higher than at the lidar cloud top and the pressure of SWIR AMVs is 54 hPa higher.

The important question now is where AMVs should be located relative to the lidar cloud top as the AMVs may represent the wind in a layer that is beneath the lidar cloud top. In that case, the AMV height should actually be lower than the lidar cloud top observations. For this reason, we computed the mean VRMS differences between the AMVs used in Fig. 3 and layer-averaged dropsonde winds to aid the interpretation of systematic height differences. Once, the dropsonde wind is averaged over a layer starting at the AMV height and going downward by 50, 100 or 150 hPa (also referred to as comparing or assigning a layer beneath hereafter) and secondly, the wind is averaged over a layer of the same depth centered at the original AMV height. Mean VRMS differences are calculated as the mean of the square-root of the sum of the squared differences of both wind components. Fig. 4 shows the relative reduction of mean VRMS differences when a layer beneath the AMV height is compared instead of a layer of the same depth around the AMV height.

For VIS AMVs, the mean dropsonde-AMV VRMS difference is always lower when dropsonde winds are averaged over layers beneath the original AMV height than over layers of the same depth centered at the original AMV height (Fig. 4). The reduction is significant at a 99% confidence level for layer depths of 50, 100 and 150 hPa using a Student's t-test for dependent samples. The largest relative reduction (18%) is reached when dropsonde winds are averaged over a vertical layer of 150 hPa that is beneath the original AMV height instead of a layer centered at the original AMV height. This indicates that VIS AMVs are clearly too high as the center of this layer is 75 hPa beneath the original AMV height and, on average, 56 hPa beneath the lidar cloud tops.

The differences of SWIR AMVs and dropsondes are also slightly reduced when dropsonde winds are averaged over layers of 100-150 hPa beneath the original AMV height instead of layers around the AMV height although those AMVs are already located 54 hPa beneath lidar cloud tops on average. The AMV-dropsonde differences for IR AMVs is slightly reduced for 50-100 hPa layers beneath the original AMV height, but slightly increased for a 150 hPa layer beneath. However, the reduction (or increase) of mean VRMS differences is generally small and not significant for IR and SWIR AMVs.

Overall, we conclude that AMV heights should be located lower than lidar cloud tops. VIS AMVs are on average located 19 hPa above lidar cloud tops, but they appear to represent winds in a layer that is centered 75 hPa lower than their current height and therefore 56 hPa lower than lidar cloud tops. IR and SWIR AMVs are already located 14 and 54 hPa beneath lidar cloud tops, respectively.

The relative reduction of AMV-dropsonde mean VRMS differences is even larger when calculated relative to differences at a discrete level, but these values may be misleading as differences are generally smaller for layer-averaged sounding winds than at a discrete level (see section 4 for further discussion on this topic).

b. Height correction

This section describes the correction of AMV heights with airborne lidar cloud top observations and the evaluation of wind differences to dropsondes before and after the height correction. The height correction shifts the AMV wind vertically to a layer relative to the height of a nearby lidar cloud top observations (see section 2 for description of data set and selection criteria). Fig. 5 shows the differences of AMV (VIS, IR and SWIR combined) and dropsonde winds using different layer depths and three different layer positions relative to the lidar cloud top observations for the correction. Mean VRMS differences generally decrease with increasing layer depth. The lowest mean VRMS difference is reached when AMVs are shifted to a layer from the lidar cloud top to 150 hPa beneath or, in other words, when AMV winds are compared to dropsonde winds averaged over a layer from the lidar cloud top to 150 hPa beneath. The bias is less than 0.2 m s^{-1} for all layer depths and position that were tested. AMV winds are on average 0.1 m s^{-1} lower than dropsonde winds when assigned to a distinct level (which corresponds to a layer depth of 0 hPa in Fig. 5) of the lidar cloud top observation and about 0.1 m s^{-1} higher when assigned to a 100-150 hPa deep layer beneath the lidar cloud top. Results for the individual channels (VIS, IR and SWIR, not shown) are similar and in general it seems best to assign AMVs to 100-150 hPa deep layers beneath the lidar cloud.

Fig. 6 shows the relative improvement, i.e. relative reduction of mean VRMS differences between AMV and dropsonde winds for assigning AMV winds to a layer of 100 or 150 hPa beneath the lidar cloud top observation instead of a layer of the same depth centered at their original height. On average, this height correction reduces VRMS differences by about 8%. Using 150 hPa layers, VRMS differences are reduced for all channels. The reduction is significant at the 99% confidence level for the whole data set, at the 95% confidence level for the SWIR AMV subset and at the 90% confidence level for the VIS AMV subset. The reduction of the IR AMV subset is not significant.

Using 100 hPa layers, there is a slight deterioration of SWIR AMV subset with the lidar-AMV height correction, but the deterioration is not statistically significant. The average improvement with 100 hPa layers is similar to the results with 150 hPa and the reduction is significant at a 95% confidence level. The VRMS reduction of the VIS AMV subset is even larger with 100 hPa layers and significant at the 95% confidence level. IR AMVs are also improved with the lidar-AMV height correction using 100 hPa layers, but results are not significant.

4. Comparing AMVs to layer-averaged radiosonde and dropsonde winds

Section 3a suggests that the error of VIS AMVs is substantially reduced when they are assigned to a layer beneath their original height and section 3b demonstrates that the error of AMVs in all channels is reduced when a layer beneath lidar cloud top observations is assigned to them. These results motivated a further investigation of how deep the atmospheric layer is that AMVs represent and how this layer should be positioned vertically. To increase the sample size, this section uses dropsondes from all four T-PARC aircraft and also special T-PARC radiosondes. The use of radiosondes also allows comparing AMVs at altitudes of 100-500 hPa, whereas the section 3 only uses AMVs beneath 500 hPa.

VB2009 already compared VRMS differences between AMV winds and layer-averaged sounding winds for layers of different depth from the AMV height downward. Their results suggest that the treatment of AMVs as layer-averaged winds beneath their original height in data assimilation could lead to a significant improvement. This section intends to complement the study of VB2009 by testing different positions of the layer relative to the original AMV height and by investigating the effect on the wind speed bias in addition to mean VRMS differences.

Assigning a layer beneath the original AMV height would result in a systematic height reduction and may therefore also introduce systematic wind errors in case the height was correct or too low before. A larger averaging volume additionally leads to lower wind speeds. As data assimilation systems are particularly sensitive to systematic errors, we investigate the wind speed bias in addition to VRMS differences and we shift the averaging layers from 50 or 100 hPa above the AMV height to 100 hPa beneath. In case the averaging layer would be beneath or partly beneath the ground, we use the lowest possible layer instead. The intention for shifting the layer is to find the optimal position of the layer relative to the AMV height and also to detect if the reduction of the difference is due to compensating systematic height errors by extending the layer to the correct height of the AMV wind or to the fact that AMVs really represent a layer wind.

The VRMS differences and the wind speed bias between AMV winds and layer-averaged sounding winds is shown in Fig. 7 for different layer depths (different line types) and as a function of the vertical offset of the center of the averaging layer relative to the AMV height. The line type with the lowest minimum indicates the optimal (or appropriate) layer depth concerning mean VRMS or wind speed bias and the position of this minimum on the x-axis the optimal (or appropriate) position of this layer relative to the AMV height. The fact that the line with the lowest VRMS minimum is also the one with the lowest VRMS value at x=0 hPa in all panels indicates that the compensation of systematic height errors is not the main effect for the VRMS reduction.

The results for IR AMVs above 499 hPa indicate that the lowest mean VRMS difference is reached when these AMV assigned to a 100 hPa layer centered ~20 hPa beneath their original height. Deeper or shallower layers both lead to larger differences. However, a 50 hPa layer centered 16 hPa beneath the original AMV height may be the best choice in case a low wind speed bias is particularly important.

AMVs beneath 500 hPa (Figs. 7b-f) generally show a less distinct minimum of VRMS differences, presumably due to lower vertical wind gradients at lower levels. The lowest mean VRMS differences are generally reached for the deepest layer that is shown, i.e. for 200 hPa. Averaging over these layers however leads to an increase of the wind speed bias that may not be desirable for data assimilation purposes. Thus, the choice of the optimal (appropriate) layer e.g. for data assimilation purposes is to some extend a trade-off between mean VRMS and bias.

The mean VRMS difference is systematically reduced by 0.2-0.4 m s^{-1} when AMVs are assigned to a 100 hPa layer centered at their original height instead of a 10 hPa layer centered at that height (upper part in Table 1). Assigning such a layer also does not seem to lead to a significant increase of the wind speed bias. Table 1 also lists the mean VRMS and bias difference for one subjectively chosen optimal layer for every panel of Fig. 7 (lower part in Table 1). 150 and 200 hPa layers were not selected due to the increase of the wind speed bias mentioned above. It is notable that these optimal layers are sometimes centered above and sometimes beneath the original AMV height in contrast to the assumption of VB2009 that layers beneath the AMV level are appropriate. The results in Fig. 7 suggest that a layer centered at the AMV height may be the best choice for all IR AMVs and for VIS and SWIR AMVs above 799 hPa. Only for VIS and SWIR AMVs beneath 800 hPa, there is indication that assigning a 100 hPa layer beneath the original AMV height is more appropriate as both the mean VRMS and bias are reduced. For VIS AMVs beneath 800 hPa such a layer beneath the original height even leads to lower VRMS differences than a layer at the original AMV height while the wind speed bias is about the same. For SWIR AMVs beneath 800 hPa, mean VRMS and bias for the layer beneath are comparable to the values for the layer centered at the original AMV height.

5. Discussion and summary

This study compares lower tropospheric AMV heights with airborne lidar cloud top observations, corrects AMV heights with these lidar cloud top observations and investigates if AMVs rather represent winds in a layer instead of at a distinct level. The field campaign T-PARC in the western North Pacific offered a unique opportunity for such an investigation as it provided hourly MTSAT AMVs produced by CIMSS, airborne lidar observations from 24 flights of the DLR Falcon, more than 300 dropsondes from the same flights for an independent evaluation of the AMV height correction using lidar observations and several thousand additional soundings for the comparison of AMVs to layer-averaged winds. The lidar-AMV height comparison and correction are limited to AMVs beneath 500 hPa due to the aircraft flight altitude, whereas the layer comparison also includes AMVs up to 100 hPa.

The height comparison of lidar cloud top observations and lower tropospheric AMVs revealed that T-PARC VIS AMVs were on average 19 hPa above the lidar cloud tops. This is consistent with the findings of Di Michele et al. 2012 that low-level AMV heights are on average higher than cloud tops derived from CALIPSO. IR and SWIR AMVs in contrast were located 14 and 54 hPa beneath lidar cloud tops, respectively. The comparison of the same VIS AMVs to nearby dropsonde winds indicated that VIS AMVs are substantially too high while no clear evidence for a height offset was found for IR and SWIR AMVs. We therefore conclude that AMV heights should actually be lower than lidar cloud top observations.

As next step, AMVs were vertically reassigned to layers of different depth and different position relative to nearby lidar cloud top observations. The best match of AMV and dropsonde winds was found when AMVs were assigned to 100 or 150 hPa deep layers beneath the lidar cloud tops. Such a height correction reduced the mean VRMS differences between AMVs and dropsonde observations by 8% in comparison to assigning AMV winds to a layer of the same depth centered at the original AMV height.

For VIS AMVs, an even larger reduction of VRMS differences to dropsonde winds by 18% was reached when AMVs were assigned to a 150 hPa layer beneath the original AMV heights. However, such a correction may not lead to same result for other AMV data sets as systematic errors strongly depend on the processing, satellite, geographic region and other factors. The lidar cloud top observations in contrast are independent of the original AMV height assignment. Therefore, the lidar correction can be expected to be applicable to other data sets (e.g. using CALIPSO satellite lidar observations) and in addition to the error reduction it can be expected that the horizontal error correlation of AMVs is reduced by incorporating such an independent data set.

The second part of the study compares AMV winds to layer-averaged radiosonde and dropsonde winds from T-PARC. Several layers of different depth are tested and these layers are shifted from above to beneath the AMV to investigate the depth of the layer that AMV winds represent and the appropriate position of such a layer relative to the original AMV height. It is found that the VRMS differences are reduced by 5-10% when AMVs are assigned to a 100 hPa layer centered at their original height in comparison to a 10 hPa layer. Layer depths of 150-200 hPa lead to a slight further reduction of VRMS errors, but also tend to increase the bias of AMV-dropsonde wind speed differences. In general, it is not completely clear how this layer should be positioned relative to the original AMV height – and this may also depend on the individual data set. As best guess based on the results of this study, we suggest assigning a 100 hPa layer centered at the AMV height to all IR AMVs and to VIS and SWIR AMVs above 800 hPa. For low-level VIS and SWIR AMVs in contrast, there is indication that it is more appropriate to assign a 100 hPa layer beneath the original AMV height.

In summary, we conclude that AMV errors could be reduced by about 5-10% when AMVs were assigned to 100 hPa layers centered at their original height. Further error reduction by 5-10% could be reached when lower tropospheric AMVs were assigned to a 100 or 150 hPa layer beneath nearby airborne lidar cloud top observations. However, it should be noted that our study only uses AMVs derived with a particular algorithm and results may differ to some extend for other AMV data sets. The height correction with lidar observations is also expected to be applicable using satellite observations, but determining the height of semi-transparent cirrus clouds from lidar observations is expected to be more difficult than the ones of opaque water clouds that were dominant in this study.

Our findings generally confirm that AMVs rather represent winds in a tropospheric layer than at a discrete level as demonstrated by VB2009 and emphasizes that AMVs should be assimilated as layer-wind in NWP models. Depending on the AMV channel and the geographical region, VB2009 suggest 50-150 hPa as appropriate layer depth for VIS, IR and

SWIR AMVs, which is on average similar to our findings despite the different data set and methodology. In addition to VB2009, we demonstrated that treating AMVs as layer winds has no negative effect on systematic errors unless the averaging layers are significantly thicker than 100 hPa. One difference is that our study suggests optimal averaging layers centered at the original AMV height for upper- and mid-level AMVs, whereas VB2009 only considered layers from the original AMV downward. Based on our findings, such layers beneath the original height may be appropriate for low-level AMVs, but tend to increase systematic errors of AMVs above 800 hPa.

Acknowledgements

AMV, lidar and dropsonde observations were made as part of T-PARC, TCS-08, and DOTSTAR. T-PARC and TCS-08 were sponsored by an international consortium from the United States (National Science Foundation, Office of Naval Research, Naval Research Laboratory, and U.S. Air Force), Germany (DLR, Forschungszentrum Karlsruhe), Japan (Japan Meteorological Agency), Korea (National Institute of Meteorological Research), and Canada (Environment Canada). The role of the National Center for Atmospheric Research's Earth Observing Laboratory (NCAR EOL) for campaign and data management is acknowledged. DOTSTAR is funded by the National Science Council of Taiwan, the United States Office of Naval Research, and the Central Weather Bureau Taiwan.

Particular thanks are due Oliver Reitebuch, Martin Wirth and Christoph Kiemle from the lidar group of the DLR Institute for Atmospheric Physics who supported the analysis of lidar observations and to the group of Chris Velden at CIMSS for processing the AMVs.

This study was carried out in the Hans Ertel Centre for Weather Research. This research network of Universities, Research Institutes and Deutscher Wetterdienst is funded by the BMVBS (Federal Ministry of Transport, Building and Urban Development).

REFERENCES

Bormann, N., S. Saarinen, G. Kelly, and J-N. Thépaut, 2003: The spatial structure of observation errors in atmospheric motion vectors from geostationary satellite data. *Mon. Wea. Rev.*, **131**,706-718.

Bormann, N. and J.-N. Thépaut, 2004: Impact of MODIS polar winds in ECMWF's 4DVAR data assimilation system. *Mon. Wea. Rev.*, 132, 929-940.

Di Michele, S., T. McNally, P. Bauer, and I. Genkova, 2012: Quality assessment of cloud-top height estimates from satellite IR radiances using the CALIPSO lidar. *IEEE Trans. Geosci. Remote Sens., accepted.*

Harnisch F., M. Weismann, C. Cardinali, and M. Wirth, 2011. Assimilation of DIAL water vapour observations in the ECMWF global model. *Quart. J. Roy. Meteor. Soc.,* **137,** 1532–1546.

Gelaro, R., R. H. Langland, S. Pellerin, and R. Todling, 2010. The THORPEX observation impact inter-comparison experiment. *Mon. Wea. Rev.,* **138,** 4009-4025.

Folger, K., 2012: Höhenkorrektur von Satelliten-Windvektoren (AMVs) mit flugzeuggetragenen Lidarmessungen. Master thesis. Ludwig-Maximilians-Universität

München, Germany. Online available at: http://www.meteo.physik.uni-muenchen.de/dokuwiki/doku.php?id=lscraig:herz:publications_en

Nieman, S. J., J. Schmetz, and W. P. Menzel, 1993: A comparison of several techniques to assign heights to cloud tracers. Journal of Applied Meteorology, **32**, 1559-1568.

Olander, Z., 2001: UW-CIMSS satellite-derived wind algorithm user's guide (version 1.n). Online available at: http://cimss.ssec.wisc.edu/iwwg/Docs/windcoug.pdf

Velden, C. S., J. Daniels, D. Stettner, D. Santek, J. Key, J. Dunion, K. Holmlund, G. Dengel, W. Bresky, and P. Menzel, 2005: Recent Innovations in Deriving Tropospheric Winds from Meteorological Satellites. *Bull. Amer. Meteor. Soc.*, **86**, 205-223.

Velden, C. S., and K. M. Bedka, 2009: Identifying the Uncertainty in Determining Satellite-Derived Atmospheric Motion Vector Height Attribution. *J. Appl. Meteor. Climatol.,* **48**, 450-463.

Weissmann M., F. Harnisch, C.-C. Wu, P.-H. Lin, Y. Ohta, K. Yamashita, Y.-H. Kim, E.-H. Jeon, T. Nakazawa, and S. Aberson, 2011. The influence of assimilating dropsonde data on typhoon track and mid-latitude forecasts. *Mon. Wea. Rev.* **139,** 908-920.

Weissmann, M., R. H. Langland, C. Cardinali, P. M. Pauley, and S. Rahm, 2012: Influence of airborne Doppler wind lidar profiles near Typhoon Sinlaku on ECMWF and NOGAPS forecasts. *Quart. J. Roy. Meteor. Soc.,* **138**, 118-130.

Wirth, M., A. Fix, P. Mahnke, H. Schwarzer, F. Schrandt, and G. Ehret, 2009: The airborne multi-wavelength water vapor differential absorption lidar WALES: System design and performance. *Appl. Phys.*, **96B,** 201-213.

	Difference of mean VRMS	Difference of absolute bias
IR, 100-499 hPa, 100 hPa layer centered at AMV	-0,36	-0,42
IR, 500-999 hPa, 100 hPa layer centered at AMV	-0,29	0,11
SWIR, 500-799 hPa, 100 hPa layer centered at AMV	-0,21	0,1
SWIR, 800-999 hPa, 100 hPa layer centered at AMV	-0,42	-0,09
VIS, 500-799 hPa, 100 hPa layer centered at AMV	-0,21	0,07
VIS, 800-999 hPa, 100 hPa layer centered at AMV	-0,24	-0,04
IR, 100-499 hPa, 50 hPa layer centered 16 hPa beneath AMV	-0,49	-0,5
IR, 500-999 hPa, 100 hPa layer centered 50 hPa above	-0,16	-0,08
SWIR, 500-799 hPa, 100 hPa layer centered 40 hPa above	-0,2	-0,38
SWIR, 800-999 hPa, 100 hPa layer centered 50 hPa beneath	-0,4	-0,11
VIS, 500-799 hPa	no suitable layer found	
VIS, 800-999 hPa, 100 hPa layer centered 50 hPa beneath	-0,44	-0,03

TABLE 1. Reduction of mean VRMS and wind speed bias (both m s^{-1}) of differences between AMV and sounding winds when sounding winds are averaged over a layer described in the left column instead of a 10 hPa layer centered at the original AMV height. Negative values indicate lower values for the layer described in left column. The upper part of the table presents the results for 100 hPa layers centered at the original AMV height, the lower part the results for one other selected layer for every panel in Fig. 7.

Figure captions

FIG. 1. (left) Location of airborne Falcon observations used in section 3; lidar observations are represented by gray lines and dropsondes by black '+'-symbols; (right) location of sounding used in section 4; black '+'-symbols mark the location of dropsondes, circles mark special T-PARC radiosondes from ships or small islands. The size of circles representing sounding stations with more than 500 AMV matches used for the comparison is scaled linearly by the number of matches; the largest circle represents 1221 matches.

FIG. 2. (a) Height distribution of AMVs used for the lidar-AMV height comparison in section 3a. (b) Height distribution of AMVs used for the height correction in section 3b.

FIG. 3. Histogram of height differences (hPa) between AMVs and lidar cloud top heights. Positive values indicate AMV heights that are lower than lidar cloud top heights.

FIG. 4. Relative reduction of mean AMV-dropsonde VRMS difference when AMVs are compared to a layer beneath the original AMV height instead of a layer centered at the original AMV height. The first three bars represent results for 50 hPa deep layers, the middle three bars for 100 hPa layers and the right three bars for 150 hPa layers.

FIG. 5. Mean VRMS and wind speed bias of differences between AMVs (VIS, IR and SWIR combined) and dropsondes when AMVs are assigned to a layer relative to nearby lidar cloud top observations. The x-axis denotes the depth of the assigned layer. The three different line types denote layers centered at the lidar cloud top (black dashed line), layers from the lidar cloud top downward (solid black line) and layers with 25% above and 75% beneath the lidar cloud top (solid gray line).

FIG. 6. Relative reduction of mean VRMS differences between AMV and dropsonde winds when AMVs are assigned to a layer beneath the lidar cloud top instead of a layer centered at the original AMV height. The depth of the layer is 100 hPa for the left bars and 150 hPa for the right ones.

FIG. 7. Mean VRMS and wind speed bias of differences between AMV winds and layer-averaged winds from dropsondes and radiosondes. The panel titles denote the AMV type (VIS, SWIR or IR), the height range of compared values in hPa and the number of compared values. Different line types represent different layer depths for the vertical averaging of dropsonde and radiosonde winds: gray dashed line for 10 hPa, gray solid line for 50 hPa, black dashed line for 100 hPa, black dash-dotted line for 150 hPa (panel (a) only) and black solid line for 200 hPa (panels (b)-(f)). Note that the scales for bias and mean VRMS values are different.

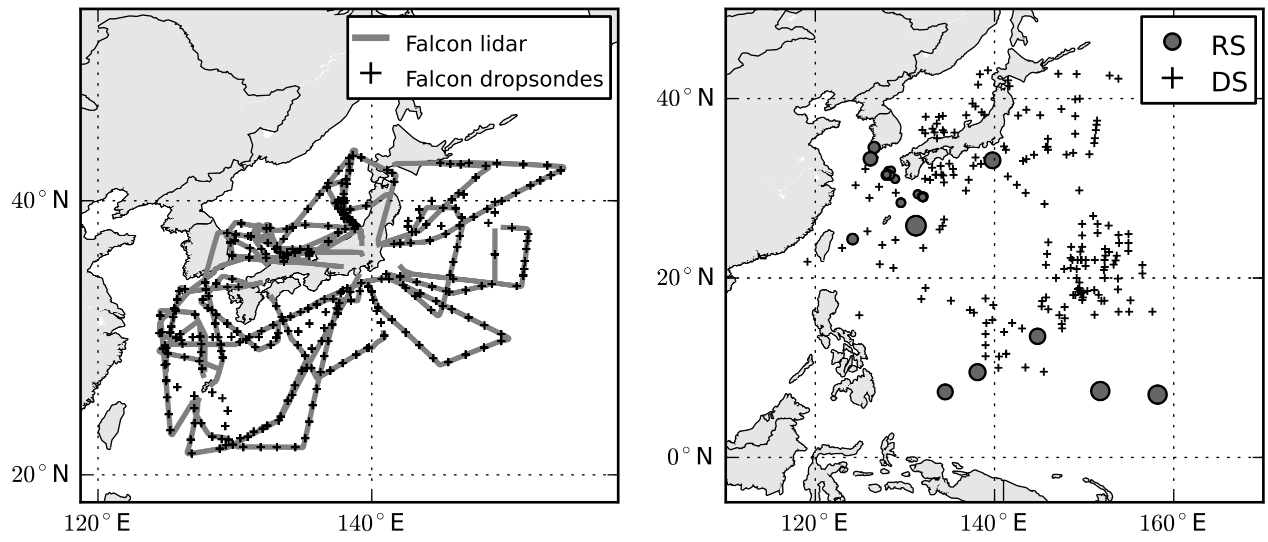

FIG. 1. (left) Location of airborne Falcon observations used in section 3; lidar observations are represented by gray lines and dropsondes by black '+'-symbols; (right) location of sounding used in section 4; black '+'-symbols mark the location of dropsondes, circles mark special T-PARC radiosondes from ships or small islands. The size of circles representing sounding stations with more than 500 AMV matches used for the comparison is scaled linearly by the number of matches; the largest circle represents 1221 matches.

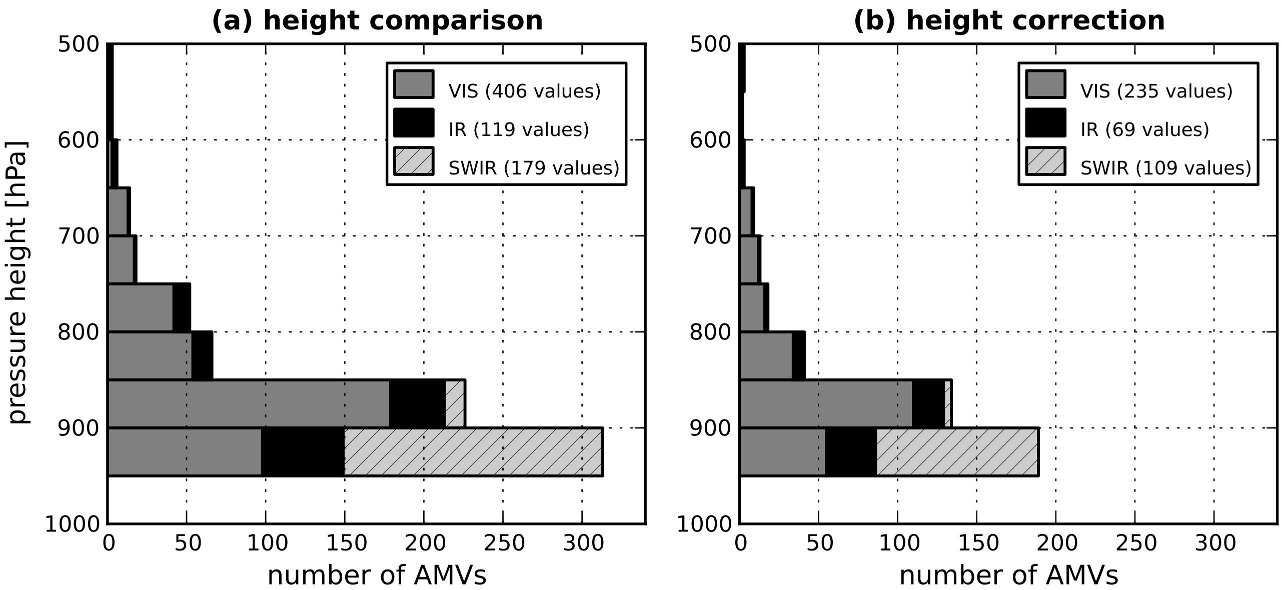

FIG. 2. (a) Height distribution of AMVs used for the lidar-AMV height comparison in section 3a. (b) Height distribution of AMVs used for the height correction in section 3b.

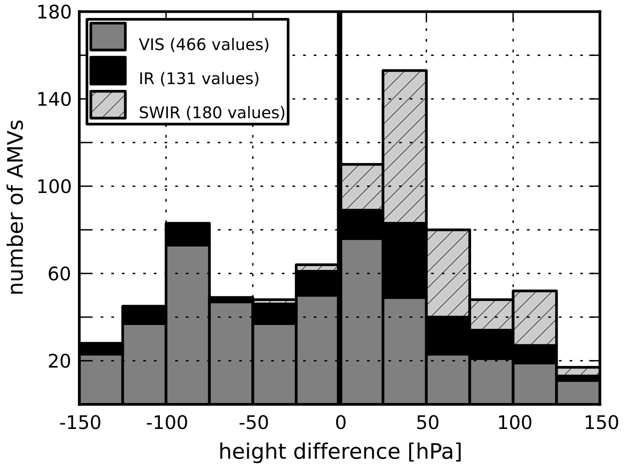

FIG. 3. Histogram of height differences (hPa) between AMVs and lidar cloud top heights. Positive values indicate AMV heights that are lower than lidar cloud top heights.

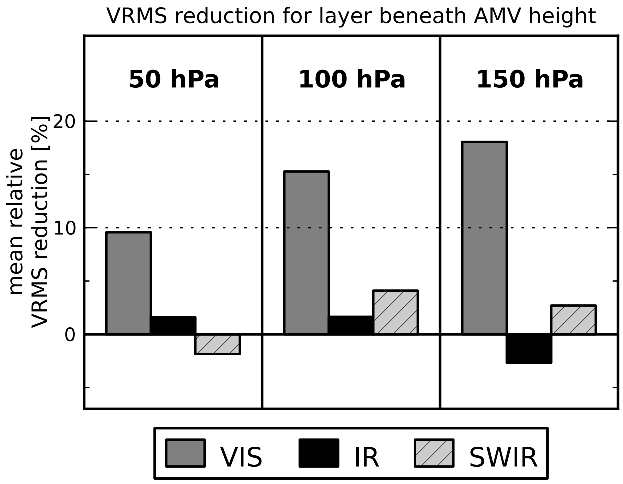

FIG. 4. Relative reduction of mean AMV-dropsonde VRMS difference when AMVs are compared to a layer beneath the original AMV height instead of a layer centered at the original AMV height. The first three bars represent results for 50 hPa deep layers, the middle three bars for 100 hPa layers and the right three bars for 150 hPa layers.

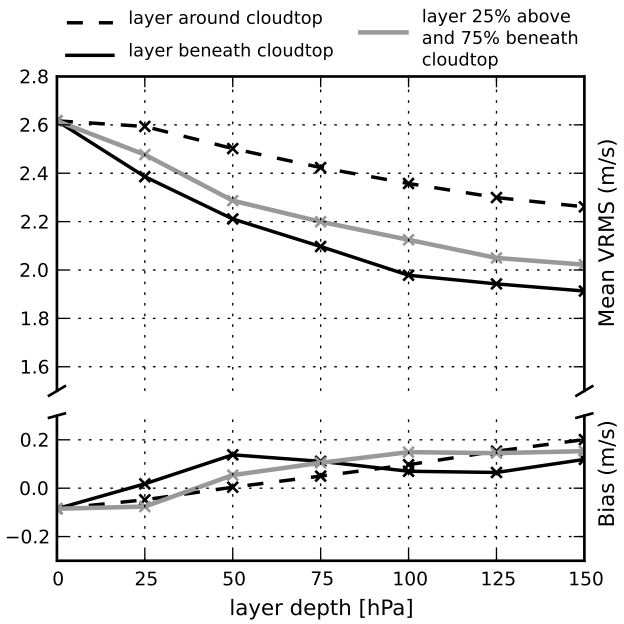

FIG. 5. Mean VRMS and wind speed bias of differences between AMVs (VIS, IR and SWIR combined) and dropsondes when AMVs are assigned to a layer relative to nearby lidar cloud top observations. The x-axis denotes the depth of the assigned layer. The three different line types denote layers centered at the lidar cloud top (black dashed line), layers from the lidar cloud top downward (solid black line) and layers with 25% above and 75% beneath the lidar cloud top (solid gray line).

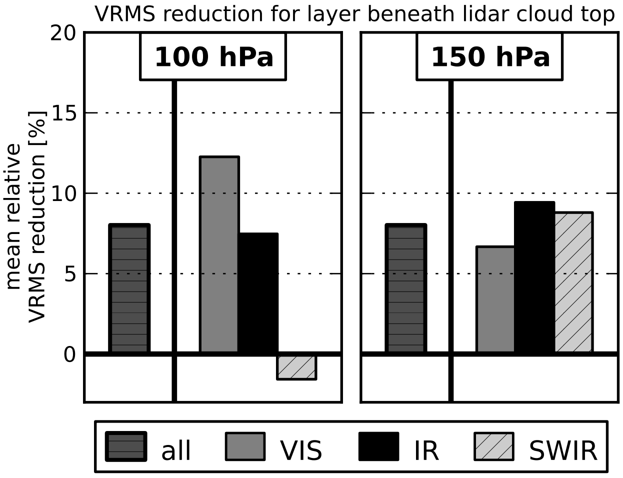

FIG. 6. Relative reduction of mean VRMS differences between AMV and dropsonde winds when AMVs are assigned to a layer beneath the lidar cloud top instead of a layer centered at the original AMV height. The depth of the layer is 100 hPa for the left bars and 150 hPa for the right ones.

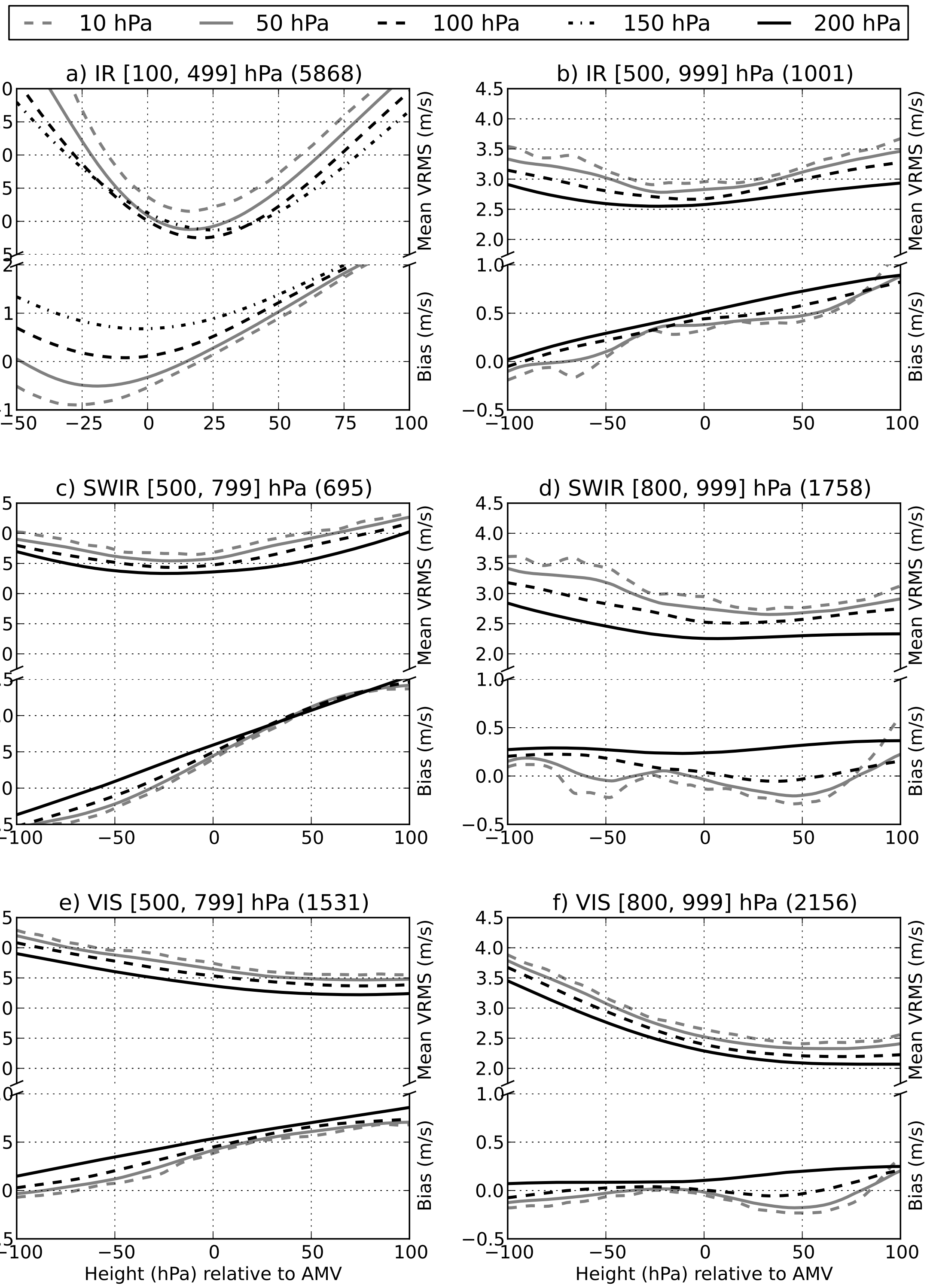

FIG. 7. Mean VRMS and wind speed bias of differences between AMV winds and layer-averaged winds from dropsondes and radiosondes. The panel titles denote the AMV type (VIS, SWIR or IR), the height range of compared values in hPa and the number of compared values. Different line types represent different layer depths for the vertical averaging of dropsonde and radiosonde winds: gray dashed line for 10 hPa, gray solid line for 50 hPa, black dashed line for 100 hPa, black dash-dotted line for 150 hPa (panel (a) only) and black solid line for 200 hPa (panels (b)-(f)). Note that the scales for bias and mean VRMS values are different.